Acta Oncologica, 2012; 51: 86–96

informa
healthcare

ORIGINAL ARTICLE

Minor changes in effective half-life during fractionated ^{177}Lu-Octreotate therapy

ULRIKE GARSKE[1*], MATTIAS SANDSTRÖM[2*], SILVIA JOHANSSON[3], ANDERS SUNDIN[4], DAN GRANBERG[5], BARBRO ERIKSSON[5] & HANS LUNDQVIST[6]

[1]*Department of Radiology, Oncology and Radiation Science, Department of Medical Sciences, Section of Nuclear Medicine, Uppsala University Hospital, Uppsala, Sweden,* [2]*Department of Oncology, Radiology and Radiation Science, Section of Medical Physics. Uppsala University Hospital, Uppsala, Sweden,* [3]*Department of Radiology, Oncology and Radiation Science, Section of Oncology and Nuclear Medicine, Uppsala University Hospital, Uppsala, Sweden,* [4]*Department of Radiology, Karolinska Institute, Stockholm and Uppsala University Hospital, Sweden,* [5]*Department of Medical Sciences, Section of Endocrine Oncology, Uppsala University Hospital, Uppsala, Sweden and* [6]*Uppsala University, Department of Oncology, Radiology and Radiation Science, Rudbeck Laboratory, Uppsala, Sweden*

Abstract

Aims. Fractionated ^{177}Lu-DOTA-octreotate therapy has been reported to be an effective treatment option for patients with generalized neuroendocrine tumors. In our clinic, full individual dosimetry is performed during the first therapy cycle, while dosimetry at later cycles is based on the 24 h uptake measurement assuming an unchanged effective half-life. Our aim was to evaluate this assumption and the variation in the 24 h uptake during therapy. *Patients.* Thirty patients, 13 women and 17 men, were included in the study. *Methods.* During the first therapy cycle the ^{177}Lu-concentration was measured with SPECT/CT over the abdomen at 24 h, 96 h and 168 h after infusion. The effective half-life was determined for the kidneys, liver and spleen. The procedure was repeated at cycle 4 or 5. *Results*. The median ratio between the effective half-lives of the latter and the first cycle was 0.97 and 1.01 for the right and left kidney, with a range of 0.89–1.01 (1st–3rd quartile) and 0.93–1.05, respectively. *Discussion.* The mean value of the ratios was slightly lower than one, indicating a tendency towards increased activity elimination during therapy. In individual patients, significant changes were found for all organs, often when a large tumor burden reduction occurred during treatment. Possible contributing factors appeared to be larger amounts of non-tumor bound tracer, improved organ function (kidneys), decrease of vessel obstruction (spleen), less scatter from large tumors and reduction of small metastases (liver and spleen). *Conclusion.* With most patients it is safe to estimate absorbed doses to kidneys, liver and spleen from 24 h activity concentration assuming an unchanged effective half-life during therapy. Patients with risk factors for kidney dysfunction need to be monitored in more detail. Simplified dosimetry based on the assumption of unchanged effective half-life can function as guidance to the number of therapy cycles an individual patient can tolerate.

Individual dosimetry is essential in all radiation therapy as a tool to obtain the highest tumor absorbed dose with an acceptable hazard for acute (deterministic) or delayed (stochastic) radiation related damage in organs at risk. This is also true in targeted radionuclide therapy (TRT). For this new evolving medical field, accurate dosimetry is more difficult to obtain than in external beam radiation, and the relation between absorbed dose and therapy effects is complex and widely unexplored. Since the dosimetry in TRT requires several measurements during a period of about a week in order to collect necessary information about kinetic changes in the radionuclide uptake, it is trying for the patient and resource demanding, if repeated at every treatment cycle.

In our clinic ^{177}Lu-DOTA-octreotate therapy is given in three to eight fractions aiming for an accumulated absorbed dose not exceeding 23 Gy to the kidneys [1–3]. In order to minimize the number of imaging cycles, only the first therapy cycle is

*Both authors contributed equally to the manuscript
Correspondence: M. Sandström, Uppsala University Hospital, Department of Medical Physics, 751 85 Uppsala, Sweden. E-mail: mattias.sandstrom@akademiska.se

(Received 10 June 2011; accepted 24 August 2011)

ISSN 0284-186X print/ISSN 1651-226X online © 2012 Informa Healthcare
DOI: 10.3109/0284186X.2011.618511

evaluated with complete dosimetry using SPECT/CT as previously described [4]. During the following cycles, the absorbed dose is estimated from one SPECT/CT measurement 24 h after infusion of the tracer, assuming an unchanged effective half-life for the particular organ. If, according to the first dosimetry, the accumulated doses in the kidneys and bone marrow would allow for more than four cycles and the treatment appears to be of clinical benefit to the patient, another complete dosimetry will be performed at cycle 4 or 5.

In this article, we report the findings regarding effective half-life, activity concentrations and calculated absorbed doses to kidneys, clinically tumor free liver, spleen and tumor in cycle 1 compared to cycle 4 or 5 based on SPECT/CT data.

In earlier published [2,5–8] data on kidney toxicity, it was concluded that the biologic effective dose (BED) is probably more relevant for the clinic than the absorbed dose. However, even use of BED requires an accurate knowledge of the absorbed dose. Using absorbed doses to the kidneys in the way we report here, will in many patients still result in more than four treatment cycles that have been earlier reported for treatment with ^{177}Lu-DOTA-octreotate [9,10].

During the last years, new possibilities have emerged regarding the methods for calculation of the absorbed dose to solid organs and tumors, e.g. to use Monte Carlo calculations to determine the energy deposit [11–13]. However, a recent publication using ^{177}Lu indicated that Monte Carlo simulation did not add significantly to the accuracy of the dose calculation [14]. This is mainly due to decay of ^{177}Lu, which emits 100% low energy beta (mean energy 133.5 keV) and 20% gamma radiation (7% 113 keV and 13% 208 keV) [15]. Therefore, we applied a previously published absorbed dose calculation method considering only local absorption in solid organs with high activity uptake [4].

The primary aim of the present work was to evaluate the assumption that the organ effective half-life is unchanged during ^{177}Lu-DOTA-octreotate therapy. A secondary aim was to evaluate the variation in the 24 h uptake measurements and the potential error in the estimation of the absorbed doses to solid organs when assuming an unchanged effective half-life.

Material and methods

Patients

Thirty patients (13 female and 17 male) with somatostatin receptor-expressing neuroendocrine tumors were included. They were treated with ^{177}Lu-DOTA-Tyr-3-octreotate, where the radioactivity was obtained from IDB, Petten, Netherlands, and the peptide was a generous gift of Professor Eric Krenning, Rotterdam. All patients in the study had shown clinical benefit after the first cycles of treatment. The inclusion criteria, administration of activity, calibration of measurements and volume of interest (VOI) analysis have been described earlier [4]. For kidney protection, beginning half an hour before the infusion of ^{177}Lu-DOTA-octreotate (7.4 GBq for every cycle) all patients received at least 1 l of commercially available 85 g amino acid mixture during 4 h, containing 6.8 g lysine and 8.4 g arginine (Vamin 14 gN/l, electrolyte-free). Four patients had undergone splenectomy before start of ^{177}Lu-DOTA-octreotate.

All patients received the same amount of amino acids at the first and latter treatment, with the exception of patient 1, who received 2 l at the first treatment and only 1 l at treatment 5, when the second dosimetry was performed. During the first and one of the later (4th or 5th) therapy cycles the patients were imaged by SPECT/CT at 24 h, 72 h and 168 h in order to obtain full dosimetry information of solid organs at risk. In the special case of peptide radiotherapy it has already been pointed out that the kidney, not the bone marrow is the main dose limiting organ [16]. Bone marrow dosimetry was also performed in this patient group and will be the topic of a forthcoming report.

Treatment intervals were six to eight weeks, with exception for patients with significant decrease of white blood cell counts and/or platelets. For those patients, the nadir was awaited after which next cycle was given as soon as possible. Patient 24 had a hemihepatectomy after cycle 2, which prolonged the interval between treatments slightly.

Imaging

Single-photon emission computed tomography (SPECT)/CT was acquired over the upper abdomen including the entire organs at risk (kidneys, liver and spleen). Imaging was performed on an Infinia (International General Electric, General Electric Medical Systems, Haifa, Israel) dual-headed gamma camera equipped with 3/8" thick NaI(Tl)-crystals with VPC-5 (MEGP) collimators. Around the dominant gamma ray energy of ^{177}Lu (208.4 keV) an energy window of 20% was used in the measurements applying 120 frames with 30 s exposure time per frame. The attenuation map was created with a four slice CT-scanner (Hawkeye, 140 kV, 3.0 mA and half rotation).

All SPECT data were reconstructed using the OSEM (Ordered Subsets Expectation Maximization) algorithm included in the Xeleris 2.0 workstation

with default settings (iterative reconstruction with eight subsets and four iterations followed by a Hann filtering with a cut-off of 0.85 cycles/cm). The analysis of the SPECT images was carried out both on a Xeleris 2.0 workstation (visual analysis) and on a HERMES workstation using inhouse implemented software.

CT analysis

For response evaluation, CT images were acquired over the abdomen and thorax, usually at baseline, before therapy cycle 3 and 5 in late arterial and venous contrast enhancement phase. 1 mm evaluation was performed according to RECIST criteria [17]. In order to evaluate changes in tumor volume, calculations were performed like this: All measurable tumor was identified and the largest diameter (D) according to RECIST established. The tumor volume was assumed to be described by a sphere with the measured diameter (D) from the RECIST evaluation. In patients with significant hepatic tumor involvement, the liver volume was calculated as an ellipsoid, with largest diameters in coronal (D_{cor}), transversal (D_{trans}) and sagittal (D_{sag}) views.

Calculation of effective half-life

The sensitivity in the SPECT measurements was estimated by imaging a spherical calibration source (100 ml) with a known activity concentration. The activity concentrations in the various organs (kidneys, liver, spleen and tumor) were calculated assuming a tissue density of 1 g/cm^3.

After the infusion of tracer, the activity concentrations were measured at 24 h, 72 h and 168 h after the start of administration. The data were fitted to a single exponential function (Equation 1)

$$C_t = C_o * e^{-\frac{\ln(2)*t}{t_{eff}}} \quad (1)$$

where:

C_t is the activity concentration at time t.

C_0 the activity concentration at time zero obtained from the curve fit.

t_{eff} the effective half-life in therapy obtained from the curve fit.

To determine how good the correlation was between the data and the fit to the single exponential function the coefficient of determination (R^2) was calculated.

The effective half-lives obtained from the first and the latter therapy cycles were denoted t^1_{eff} and t^4_{eff}, respectively.

Calculation of cumulative activity concentration

The time-integrated activity concentration were calculated by integrating Equation 1 from time zero to infinity

$$\tilde{C} = \int_0^\infty C_o * e^{-\frac{\ln(2)*s}{t_{eff}}} ds = C_o * \frac{t_{eff}}{\ln(2)} \quad (2)$$

where

$\tilde{C}$ is the cumulative activity concentration in the organ.

The time-integrated activity concentration in the first and the latter therapy cycle was denoted as C_1 and C_4, respectively.

An alternative way to calculate the accumulated activity concentration in the succeeding therapy cycles was to use the 24 h measurement of the activity concentration (C^4_{24}) combined with the effective half-life from the first therapy cycle (t^1_{eff}) and the time of measurement (t). The activity concentration at time zero in the latter therapy cycle (C^4_0) was calculated as:

$$C^4_0 = C^4_{24} * e^{\frac{\ln(2)*t}{t^1_{eff}}} \quad (3)$$

Calculation of absorbed dose

Absorbed doses were calculated by using a simplified dosimetry method based on small VOIs as described earlier [4]. In SPECT data spherical volumes of interest (VOIs; 4 cm^3) were placed on the images over the two kidneys, liver, spleen and tumor. For each time point the radioactivity concentrations were determined as a mean in the VOIs sampling the organs. A single exponential function was fitted to the data and the cumulative activity was obtained by integrating this function from zero to infinity.

The minor ($< 2\%$ in kidneys, liver, spleen and tumor [4]) crossfire dose from gamma irradiation was neglected. A dose factor (DF) representing the standard organ size was used to compensate for the small gamma radiation contribution to the self-dose (approximately 5% [4]). The absorbed dose calculations were then reduced to a simple multiplication of the accumulated activity with an appropriate DF. The absorbed dose when full kinetic information was available was denoted as D_1 and D_4 for the first and the latter cycle, respectively. The dose calculated with the assumption of unchanged effective half-life was denoted D_{14} (Table I).

Table I. Absorbed dose for left and right kidney in early and late therapy for all 30 patients receiving 7.4 GBq. The late dose is also presented with the kinetics from therapy 1 (D_{14}).

	D_1 [Gy]		D_4 [Gy]		D_{14} [Gy]	
Patient number	Kidney Right	Kidney Left	Kidney Right	Kidney Left	Kidney Right	Kidney Left
1	2.9	2.3	3.7	2.9	3.2	2.2
2	3.6	3.3	4.5	4.4	5.0	4.3
3	3.0	3.0	3.4	3.2	4.0	3.8
4	3.9	3.1	3.9	4.7	4.3	3.4
5	4.7	4.6	3.8	3.9	4.0	4.1
6	3.7	3.3	4.4	3.9	4.5	4.0
7	5.1	4.9	5.9	5.8	6.3	5.8
8	3.8	3.0	5.0	3.9	6.7	5.0
9	4.6	4.1	3.8	3.7	4.4	3.6
10	4.0	4.0	3.9	3.7	4.1	3.7
11	3.8	4.0	3.0	3.0	2.8	3.2
12	3.5	4.2	4.3	4.5	5.4	5.1
13	3.1	2.7	2.9	2.8	2.9	2.9
14	3.5	3.0	3.4	4.0	3.6	3.9
15	2.2	2.0	2.5	2.2	2.3	1.9
16	4.6	4.9	6.8	7.0	8.5	8.8
17	4.8	4.7	4.8	4.6	5.4	5.3
18	2.3	1.7	3.1	2.9	4.2	3.4
19	3.8	3.1	4.7	4.1	5.4	4.7
20	4.9	4.0	5.1	5.0	5.4	4.8
21	3.3	2.6	4.4	4.0	6.8	4.2
22	4.0	3.7	4.8	4.7	4.8	4.9
23	3.2	3.0	4.9	5.6	5.7	5.4
24	3.1	3.3	4.8	4.7	6.2	5.0
25	4.1	3.6	4.5	4.0	4.4	4.2
26	6.3	6.4	6.8	6.9	6.8	7.0
27	4.3	4.5	3.9	3.5	3.9	3.5
28	4.0	3.7	6.0	6.0	6.3	6.0
29	4.6	4.0	4.9	4.4	5.0	4.8
30	2.9	2.7	5.1	4.9	5.5	4.5

Comparison of the latter cycle with the first cycle

The data obtained in the latter therapy cycle were divided by those of the first. Following ratios were formed:

$$R_{t_{eff}} = \frac{t^4_{eff}}{t^1_{eff}}, R_{uptake} = \frac{C^4_{24}}{C^1_{24}}, \text{and } R_{dose} = \frac{D_4}{D_1}.$$

The individual data from the 30 patients were plotted and the means, medians, 1st and 3rd quartiles of the quotients were calculated.

Statistics

The obtained data, both as absolute values and ratios were analyzed with an Andersson-Darling test in order to check for normal distribution. Since only about half of them passed the test, a non-parametric Wilcoxon paired test was applied to check for statistical significances.

Results

Comparison of the effective half-lives

The $R_{t_{eff}}$ values for different organs are documented in Figure 1 and the means, medians, 1st and 3rd quartiles are presented in Table II. The effective half-life in the kidneys and liver decreased in most of the patients during the therapy, resulting in mean ratios slightly lower than one. The variation in the data was small for the kidney and the spleen (interquartile range (IQR), 0.12 and 0.12, respectively) and somewhat larger for the tumor and liver (IQR 0.23 and 0.28). The coefficient of determination (R^2) of measured data and fits was generally high (>0.99).

The general tendency that the effective half-life in the kidney decreased during therapy is further illustrated in Figure 2 in which $R_{t_{eff}}$ of the left kidney is plotted against that of the right kidney. Most patients were clustered around 1. Some of them, however, showed a marked decrease in both kidneys. All patients with a substantial decrease of tumor burden during therapy were found in the latter group (patients 3, 8, 12 and 18, Table I, III and IV, and Figure 3). By contrast, two subjects (patients 1 and 15) showed a striking increase of t_{eff}. The first patient (no. 1) who had more than 20% increase received 2 l of amino acid infusion during the first cycle of therapy, but only 1 l during the latter cycle. She suffered from a low-proliferative neuroendocrine tumor of unknown origin with high tumor burden predominantly located to the liver. Previous cisplatinum-based chemotherapy had to cease after 12 cycles because of bone marrow toxicity. Glomerular filtration rate (GFR) and creatinine remained normal and stable throughout TRT comprising six cycles with ^{177}Lu-DOTA-octreotate.

The second patient (no. 15) with a substantial increase of t_{eff} for both kidneys by 14% and 18% (right and left kidney, respectively) had received 2 l

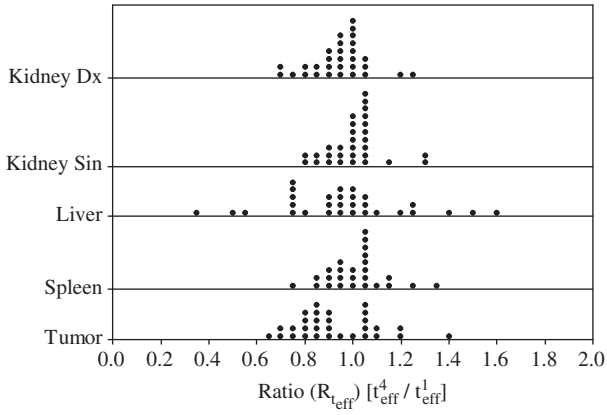

Figure 1. Dotplot of the ratios of the effective half-life between cycle 4 or 5 to cycle 1.

Table II. The statistics of the ratios of the effective half-life of the solid organs at risk in cycle 4 or 5 versus cycle 1.

Variable	Organ	N	P	1st quartile	median	3rd quartile	mean
Effective half-life	Kidney Right	30	0.014	0.89	0.97	1.01	0.95
Ratio (R_{teff})	Kidney Left	30	0.869	0.93	1.01	1.05	1.00
	Liver	30	0.188	0.77	0.96	1.05	0.96
	Spleen	26	0.879	0.94	1.02	1.06	1.01
	Tumor	30	0.017	0.82	0.89	1.05	0.93
Activity concentration	Kidney Right	30	0.001	1.00	1.14	1.32	1.17
Ratio (R_{uptake})	Kidney Left	30	0.001	1.07	1.21	1.40	1.24
	Liver	30	0.026	0.52	0.82	1.09	0.83
	Spleen	26	0.128	0.91	1.08	1.45	1.21
	Tumor	30	0.000	0.42	0.62	0.80	0.61
Absorbed dose	Kidney Right	30	0.001	1.02	1.14	1.42	1.24
Ratio (R_{dose})	Kidney Left	30	0.002	1.06	1.17	1.45	1.24
	Liver	30	0.008	0.61	0.82	1.03	0.89
	Spleen	26	0.099	0.86	1.15	1.41	1.19
	Tumor	30	0.000	0.49	0.67	0.83	0.64

of amino acid infusion during both cycles. After the first cycle this patient experienced an immediate inflammatory reaction consistent with tumor necrosis. The treatment resulted in a subsequent reduction of the tumor (37% according to RECIST up to 18 months after treatment, still decreasing) and U-5-HIAA by more than 50%. This patient also suffered from arterial hypertension and already before the treatment showed slightly elevated P-creatinine, but with a GFR within the lower normal range.

Comparison of uptake values

The R_{uptake} values for kidneys, liver and spleen are seen in Figure 4, and the means, medians, 1st and 3rd quartiles are presented in Table II. The mean R_{uptake} for kidneys and spleen increased, while it decreased in the liver. As presented in Figure 4 there was a considerable variation in the data between patients. The IQR was for the right kidney 0.32, for the left kidney 0.34, for the liver 0.58, for the spleen 0.54 and for the tumors 0.38. Patients with a substantial decrease of tumor burden showed generally increased uptake values (especially patients 8 and 24) in the kidneys. The only exception was patient 3, who experienced a tumor decrease of about 1.5 l between the dosimetry cycles.

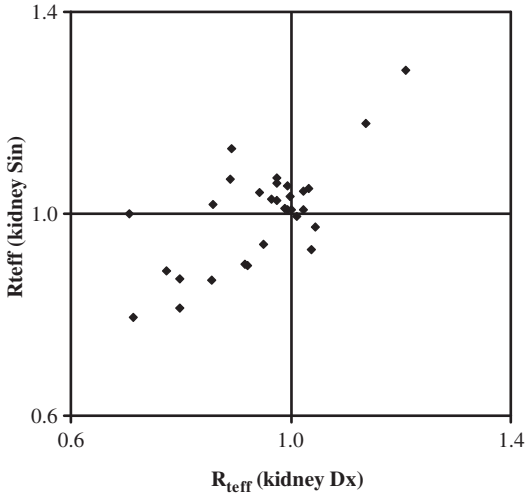

Figure 2. Comparison of the effective half-life changes in the left and right kidney during therapy.

Absorbed dose

The dot plots of the ratios between the calculated absorbed doses in the solid organs at risk are demonstrated in Figure 5. The means, medians, 1st and 3rd quartiles are shown in Table II. A similar increase of the uptake values was found in the kidneys and the spleen, while a decrease of the values was seen in the liver. The variation in these data was similar to that of the uptake values. The IQR was for the right kidney 0.39, for the left kidney 0.39, for the liver 0.42, for the spleen 0.54 and for the tumors 0.34.

Tumor size

Tumor response according to RECIST criteria in percent difference from cycle 1 to cycle 4 or 5 is presented in Table IV. In the same table the calculated volume change is also presented. Volume calculations and RECIST evaluation could not be performed in all cases due to technical issues (use of magnetic resonance imaging (MRI) during follow-up, analog images). A decrease of tumor size was seen both with RECIST (mean 45.6, IQR 32.9 and p 0.000) and with volume calculation (mean 285, IQR 295 and p 0.000).

Discussion

To optimize radiation therapy, whether with external beam, brachytherapy or thoracic radiotherapy

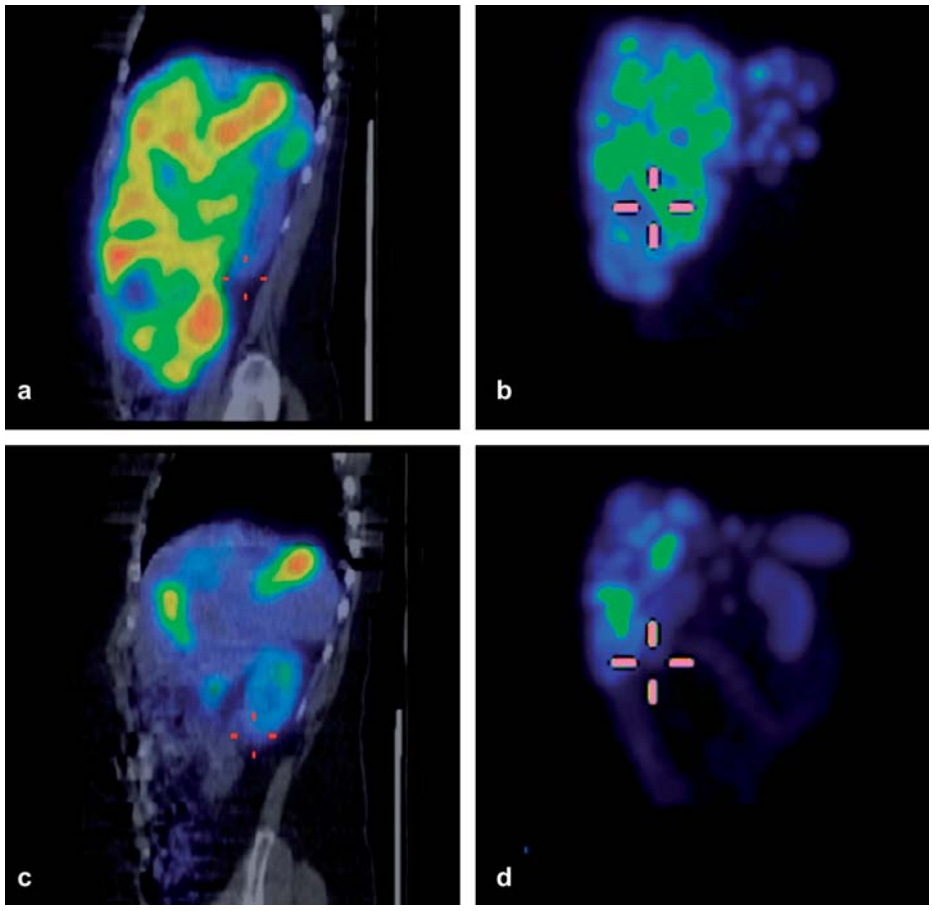

Figure 3. Example of change in tumor volume (liver metastases, hair cross on caudal pole of right kidney) during therapy in patient no. 8 (rectal carcinoid). SPECT/CT images 24 h after cycle 1 (a, b) and 6 (c, d); (a, c: fused sagittal views) b, d: maximum intensity projections.

(TRT), the absorbed doses to the risk organs and tumors in the individual patient have to be quantified with highest possible accuracy. Especially in TRT, where the organ doses may change dramatically because of altered organ function, tumor burden and altered hormone release from the tumor, individualized patient dosimetry is indispensable. It will enable a better use of the therapeutic window and improve the chances of therapeutic success. Furthermore, correct dosimetry will facilitate better prediction of therapy response and the occurrence of deterministic and stochastic radiation effects [18]. The clinic of neuroendocrine tumors in advanced stages as we see them tells, that progression and fatal outcome often is related to disseminated, small volume disease. TRT with ^{90}Y and ^{177}Lu has shown its potential in decreasing macroscopic tumor burden, but this clinical observation would be wanting for the possibility of several repeated treatments in order to treat surviving fractions of small volume disease proliferating under earlier cycles of the treatment.

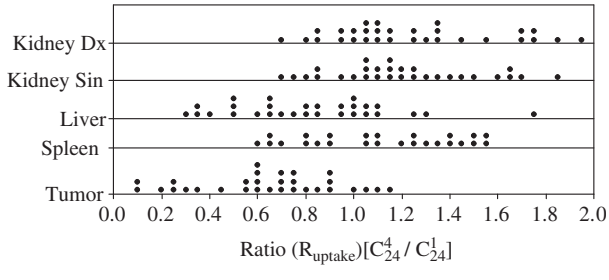

Figure 4. Dotplot of the ratios of the activity concentration after 24 h between cycle 4 or 5 to cycle 1.

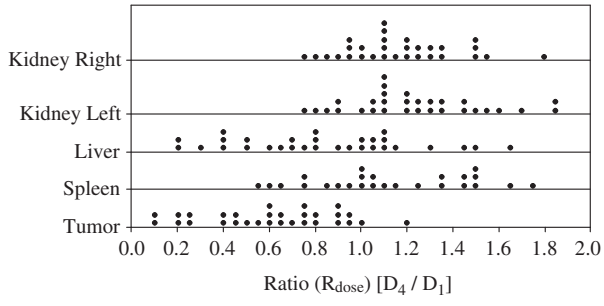

Figure 5. Dotplot of the ratios of the absorbed dose between cycle 4 or 5 to cycle 1.

Table III. Effective half-life (t_{eff}) and uptake values for left and right kidney in early and late therapy cycles.

	t_{eff} 1 [h]		C_{24} 1 [MBq/ml]		t_{eff} 4 [h]		C_{24} 4 [MBq/ml]	
Patient number	Kidney Right	Kidney Left	Kidney Right	Kidney Left	Kidney Right	Kidney Left	Kidney Right	Kidney Left
1	53.6	44.2	0.35	0.29	64.8	56.8	0.37	0.30
2	55.9	53.2	0.40	0.38	54.4	57.1	0.53	0.49
3	55.5	59.6	0.36	0.32	47.5	51.8	0.40	0.36
4	76.7	60.8	0.34	0.32	68.3	68.6	0.36	0.36
5	44.7	44.5	0.62	0.62	44.2	45.0	0.51	0.53
6	44.6	43.4	0.50	0.46	45.6	45.3	0.61	0.55
7	51.3	50.4	0.59	0.57	50.0	51.7	0.75	0.71
8	70.6	62.7	0.35	0.31	50.4	49.8	0.54	0.46
9	55.5	52.7	0.52	0.49	55.1	53.2	0.48	0.41
10	50.2	46.5	0.48	0.49	50.2	46.9	0.49	0.47
11	56.7	60.9	0.44	0.43	58.8	56.5	0.32	0.34
12	67.8	66.0	0.34	0.39	54.1	57.5	0.48	0.47
13	53.3	54.0	0.35	0.30	53.3	55.9	0.33	0.33
14	53.3	45.5	0.40	0.39	50.3	47.4	0.50	0.65
15	47.2	43.1	0.35	0.34	58.4	55.3	0.27	0.25
16	59.5	60.2	0.48	0.50	47.5	49.0	0.83	0.85
17	47.9	48.7	0.59	0.57	44.1	43.7	0.64	0.61
18	76.0	62.7	0.20	0.16	58.7	55.6	0.34	0.32
19	54.8	49.1	0.43	0.40	50.2	44.2	0.59	0.54
20	57.6	53.2	0.57	0.51	56.2	56.3	0.57	0.55
21	66.1	48.0	0.31	0.31	46.7	48.1	0.59	0.50
22	44.7	44.4	0.55	0.52	45.2	44.2	0.63	0.64
23	59.5	49.1	0.35	0.37	53.0	52.4	0.60	0.69
24	50.8	44.1	0.40	0.43	43.5	44.9	0.68	0.64
25	51.0	50.4	0.48	0.44	53.3	49.0	0.53	0.50
26	52.0	53.4	0.75	0.75	53.2	53.9	0.78	0.79
27	46.7	46.8	0.58	0.62	48.3	49.1	0.48	0.43
28	48.7	44.7	0.51	0.52	48.3	47.1	0.70	0.73
29	58.0	54.2	0.49	0.45	55.1	50.9	0.52	0.52
30	57.9	48.5	0.31	0.33	55.9	49.9	0.57	0.54
mean	55.6	51.5	0.446	0.433	52.2	51.2	0.534	0.518
1st quartile	50.3	45.7	0.352	0.330	47.7	47.2	0.480	0.416
Median	54.2	49.8	0.435	0.433	51.7	50.4	0.530	0.511
3rd quartile	58.0	54.2	0.516	0.510	55.1	55.6	0.609	0.634

Optimal dosimetry would imply measurement of the activity distribution at each therapy cycle and application of Monte Carlo calculations to achieve the best possible quantification [11–13]. Even though the calculation time for Monte Carlo simulations could be reduced, image acquisition is both time consuming and resource demanding and may be cumbersome for the patient, as it requires several hours of immobilization. Neuroendocrine tumors still being a rare disease, treatment is concentrated to larger tumor centers. This implies often long distance journeys for the patient, and dosimetry imaging during one week after each cycle is rarely feasible. Therefore, individualized dosimetry may presently be difficult to establish as a clinical routine, and the trade-off between clinical feasibility and desirable accuracy needs to be considered.

Consequently, in our present clinical routine we have applied a pragmatic approach in order to achieve individualized dosimetry during ^{177}Lu-Octreotate TRT. During the first cycle of therapy, the activity kinetics in the organs at risk was fully characterized. During the following therapy cycles the activity uptake was measured only at 24 h and the absorbed dose was calculated by using the effective half-life as assessed during the first cycle.

In this paper, we report our findings on the stability of effective half-life and absorbed doses to kidneys, liver and spleen during fractionated treatment with ^{177}Lu-DOTA-octreotate. Our treatment aim was to administer as many cycles of ^{177}Lu-DOTA-octreotate as possible without exceeding an accumulated dose of 23 Gy to the kidneys. All patients reported here had clinical benefit of the treatment, in most cases with radiologically measurable decrease of tumor volume and/or tumor markers.

Under this precondition, the effective half-life in the kidneys remained stable or decreased in all patients but two. In the first of these patients (no. 1) this could be attributed to a higher amount of co-administered amino acids during cycle 1 than during cycle 4. Our experience from the study that

Table IV. Changes in tumor size according to RECIST and changes in tumor and liver volume: Columns 1 and 2: Difference in percent between tumor sizes at first and second complete dosimetry, and between first dosimetry and at time of best response according to RECIST criteria. Columns 3 to 6: changes in tumor and liver volumes, respectively according to simplified volume calculation model (tumors represented by spheres, summed tumor volume of all evaluable tumors according to CT; liver volume represented by an ellipsoid). Patients with abundant tumor in the liver occasionally showed initially a more marked decrease in liver volume than in tumor volume (patients 1 and 8), patient 4 showed an increase of liver volume after the first treatments, that preceded a significant volume reduction of liver metastases, and subsequent volume reduction of the liver later on during therapy. Remodeling of the liver and inflammatory reaction being potential reasons. Patient 19 underwent hemihepatectomy including resection of remnants of large liver metastasis during therapy.

	Tumor				Liver	
Patient number	RECIST at dosimetry [%]	RECIST at best [%]	Δ Volume at dosimetry [ml]	Δ Volume at best [ml]	Δ Volume at dosimetry [ml]	Δ Volume at best [ml]
1	−9.5	−23	−483	−635	−848	−646
2	−19.5	−39	−331	−504	451	491
3	−41	−89	−1466	−2012	n.a.	n.a.
4	1	−50	−172	−1432	848	−1374
5	−10	−39	−8	−25	−5	−250
6	−27.5	−39	−42	−53	−316	−360
7	n.a.	n.a.	n.a.	n.a.	n.a.	n.a.
8	−32	−53	−1589	−2032	−1329	−1281
9	−0	n.a.	−25	n.a.	n.a.	n.a.
10	−35	−38	−25	−26	−13	85
11	n.a.	n.a.	n.a.	n.a.	n.a.	n.a.
12	−43	n.a.	−298	n.a.	n.a.	n.a.
13	n.a.	n.a.	n.a.	n.a.	n.a.	n.a.
14	n.a.	n.a.	n.a.	n.a.	n.a.	n.a.
15	−30	−38	−226	−256	−162	−222
16	6	−25	16	−39	56	−290
17	−38	n.a.	−10	n.a.	−14	n.a.
18	−25	−62	−98	−152	−213	−358
19	−22	−40	−214	−333	−227	−1134
20	−27	−27	−128	−128	−806	−806
21	−14	−55	−400	−922	−425	−996
22	−17	−17	−137	−137	−424	−424
23	−12	−17	−801	−1023	−421	n.a.
24	−10	−44	−1038	−1107	−1417	−1106
25	−12	−17	−202	−268	172	−565
26	−82	−86	−34	−36	151	107
27	−16	−24	−50	−73	n.a.	n.a.
28	−20	n.a.	−26	n.a.	−110	n.a.
29	−29	−37	−327	−380	n.a.	n.a.
30	n.a.	n.a.	n.a.	n.a.	n.a.	n.a.

the commercially available amino acid solution Vamin 14 gN/l was generally well tolerated prompted us to change the therapy protocol, and now all patients receive 2 l instead of 1 l, administered during 8 h.

Animal data indicate that there is a dose relationship between the amount of administered amino acids and the absorbed dose to the kidneys [19]. Various reports, using different amino acid preparations, with various administration protocols, state that especially cationic amino acids protect the kidneys from radiation related impairment [8,20]. A dose relationship and a time dependency have been reported, with lower absorbed doses to the kidneys when prolonging/increasing the amount of the amino acid infusion [8,20]. The total amount of cationic amino acids is somewhat lower than the amount used by the Rotterdam group, but infusion of mixed amino acids during a longer time has earlier been shown to have a similar effect on the kidney uptake [21].

The second of the patients (no. 15), who showed an increase of $t_{eff,}$ had a long clinical history of arterial hypertension and a kidney function in the lower normal range. A fast increase of his U-5-HIAA, however, put him in a worse condition, since dehydration due to diarrhea potentially could decrease his kidney function. During the first cycle of TRT he showed remarkably low absorbed doses to the kidneys (2.0 Gy and 2.2 Gy to the right and left, respectively). Three cycles, each with 7.4 GBq ^{177}Lu-DOTA-octreotate, resulted in a more than 50% reduction of the U-5-HIAA, which stabilized on the lower lever after two subsequent cycles with reduced activity (each cycle 3.7 GBq). By then, the clinical status of the patient had improved, and the accumulated doses to the kidneys had not exceeded 13 Gy.

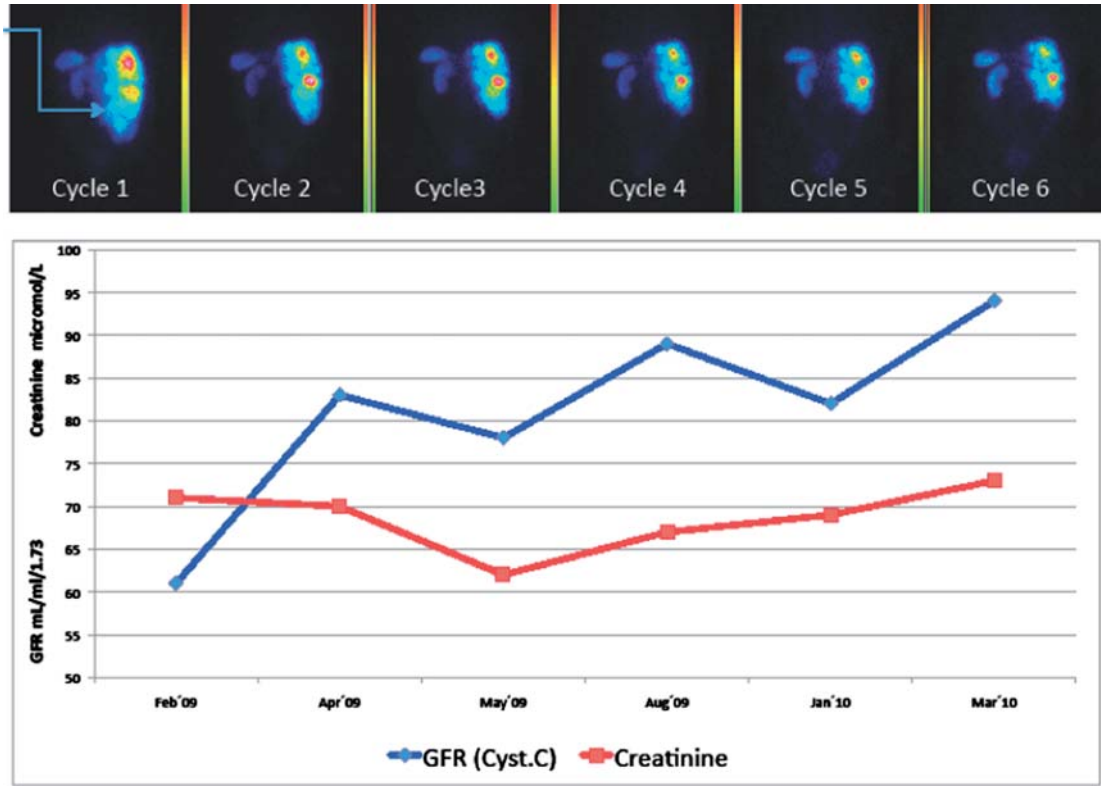

Figure 6. First row: dorsal view derived from 24 h whole body scan, cycle 1 to 6 in patient no. 8 (rectal carcinoid). Note the side difference between kidney uptake during therapy (arrow on caudal pole of right kidney at first cycle). Second row: Cystatin-C derived GFR (mL/min/1.73 m^2, normal range > 80 (age adjusted) and P-creatinine (µmol/l) at corresponding times.

After one year of follow-up, the P-creatinine was basically unchanged, and three months after the last cycle, GFR had increased from 60 to 76 ml/min. The previous findings, reported by Valkema et al. [22], of an increased risk for kidney damage in patients with arterial hypertension during ^{177}Lu-DOTA-octreotate therapy, can apply to this patient and may at least partly explain his increase of t_{eff}. In addition, the tumor necrosis seen after the first cycle of treatment may have influenced the t_{eff}. When analyzing the tumor data in correlation to the liver volume in this patient, a CT-scan five days after cycle 1 revealed an enlargement of one liver metastasis to about twice its volume of 120 ml, while the liver volume was calculated to increase with 1200 ml. Two more patients (patients 2 and 4) showed early on during therapy a swelling of the liver, that was inverse to the tumor reduction seen at that time, and that preceded significant tumor reduction, accompanied by radiological signs of necrosis later on. These findings indicate inflammatory reactions, that are hard to quantify, but may influence radiosensitivity and clinical toxicity.

These findings indicate that patients with cardiovascular risk factors, borderline kidney dysfunction, and those with dramatic decrease of tumor burden may warrant more caution. Consequently, for these patients at risk monitoring with repeated complete dosimetry has now become an established routine in our department.

By contrast, some patients improved their kidney function during therapy. This might be explained by the decrease of the tumor burden that reduced mechanical obstructions and improved blood flow. In patient 3, a substantial reduction of retroperitoneal and pelvic lymph nodes occurred during therapy, resulting in a normalized anatomy of urether and bladder, which had been dislocated by the tumor masses. Patient 8 suffered from an enlargement of the liver, causing a displacement especially of the right kidney. During the treatment, we found a steady improvement of the kidney function, mirrored by the increase of glomerular filtration rate (GFR) that was concomitant with the decrease of tumor uptake as visualized by scintigraphy (Figures 3 and 6).

In most patients, t_{eff} of the kidneys remained stable or decreased during the cycle of ^{177}Lu-DOTA-octreotate therapy, while the calculated absorbed doses increased. A combination of improved kidney function, as discussed above, and higher amounts of non-tumor bound tracer due to decreased tumor uptake to be cleared by the kidneys seems to be a reasonable explanation. Other contributing factors might be the altered impact of hormones produced by the tumors. Reduced amounts of, for example,

serotonin catabolites and insulin may have a clinical impact on the clearance of radionuclides. The detailed analysis of this is, however, beyond the scope of this article.

The effective half-life in the liver during therapy did not follow the same pattern as in kidneys and spleen, but showed a higher variability. One obvious explanation lies in the fact that most of the studied patients harbored, to different degrees, metastases in the liver. In some patients, healthy liver parenchyma was hard to distinguish from the tumor, and it was impossible to completely rule out some contribution from tumor uptake even in small volumes of interest. Additionally, the tumor response could differ substantially between patients. As Figure 3 demonstrates, occasionally a shift from a widely tumor engaged liver to an image with readily distinguishable normal liver uptake could occur under the process of treatment.

With TRT the applied tolerance doses for organs at risk are mainly derived from external radiotherapy. For the kidneys, the tolerance dose of accumulated 23 Gy thus estimated was generally found to be safe, when applied by Kwekkeboom, Krenning et al. in a study including more than 500 patients receiving a total of four treatment cycles [9,10]. Decreased kidney function following treatment with ^{177}Lu-DOTA^0, Tyr^3-octreotate was reported by the same group to occur in patients with previous kidney problems and concomitant disease that might have promoted kidney failure [22].

It has been shown that by using voxel-based calculations and assuming a homogeneous distribution within the kidney parenchyma, the tolerance dose for the kidneys during therapy with ^{177}Lu-DOTA^0, Tyr^3-octreotate might rather be about 29 Gy [23]. When we applied our small VOIs dosimetry method based on SPECT/CT [4], we found that approximately 50% of our patients were under-treated with four cycles with 7.4 GBq, in the sense that the accumulated absorbed dose to the kidneys dose did not reach 23 Gy. In our present treatment approach, we apply as many treatments as would render an accumulated dose of 23 Gy. In order to stay within safety limits we have not yet exceeded this dose limit. Only few patients had to stop due to reaching 23 Gy after only three cycles.

With most patients it is safe to estimate the absorbed doses to kidneys, liver and spleen from the 24 h activity concentration measurements and assuming an unchanged t_{eff}. For most patients, this assumption will result in a negligible error or an underestimation. In more than 90% of the patients, the simplified dosimetry used at the late therapy cycle was found to estimate the kidney dose correctly or overestimated it. At present, we find that this approach is an acceptable compromise between feasibility and precision. Patients at risk for kidney dysfunction, as well as after larger changes of tumor volume, need to be monitored in more detail. The risk-benefit for treatment must be observed for the individual patient. Simplified dosimetry, based on the assumption of unchanged t_{eff}, is sufficient to guide the number of therapy cycles that the individual patient can tolerate.

Acknowledgements

The authors would like to thank the staff at the departments of nuclear medicine, medical physics and endocrine oncology (78D) for their great assistance. The authors declare that they have no conflict of interest.

References

[1] Kwekkeboom DJ, Bakker WH, Kooij PP, Konijnenberg MW, Srinivasan A, Erion JL, et al. [177Lu-DOTAOTyr3]octreotate: Comparison with [111In-DTPAo]octreotide in patients. Eur J Nucl Med 2001;28:1319–25.

[2] Barone R, Borson-Chazot F, Valkema R, Walrand S, Chauvin F, Gogou L, et al. Patient-specific dosimetry in predicting renal toxicity with (90)Y-DOTATOC: Relevance of kidney volume and dose rate in finding a dose-effect relationship. J Nucl Med 2005;46(Suppl 1):99S–106S.

[3] Emami B, Lyman J, Brown A, Coia L, Goitein M, Munzenrider JE, et al. Tolerance of normal tissue to therapeutic irradiation. Int J Radiat Oncol Biol Phys 1991;21:109–22.

[4] Sandstrom M, Garske U, Granberg D, Sundin A, Lundqvist H. Individualized dosimetry in patients undergoing therapy with (177)Lu-DOTA-D-Phe (1)-Tyr (3)-octreotate. Eur J Nucl Med Mol Imaging 2010;37:212–25.

[5] Bodei L, Cremonesi M, Grana C, Rocca P, Bartolomei M, Chinol M, et al. Receptor radionuclide therapy with 90Y-[DOTA]0-Tyr3-octreotide (90Y-DOTATOC) in neuroendocrine tumours. Eur J Nucl Med Mol Imaging 2004;31:1038–46.

[6] Cremonesi M, Botta F, Di Dia A, Ferrari M, Bodei L, De Cicco C, et al. Dosimetry for treatment with radiolabelled somatostatin analogues. A review. Q J Nucl Med Mol Imaging 2010;54:37–51.

[7] Wessels BW, Konijnenberg MW, Dale RG, Breitz HB, Cremonesi M, Meredith RF, et al. MIRD pamphlet No. 20: The effect of model assumptions on kidney dosimetry and response – implications for radionuclide therapy. J Nucl Med 2008;49:1884–99.

[8] Rolleman EJ, Melis M, Valkema R, Boerman OC, Krenning EP, de Jong M. Kidney protection during peptide receptor radionuclide therapy with somatostatin analogues. Eur J Nucl Med Mol Imaging 2010;37:1018–31.

[9] Kwekkeboom DJ, Teunissen JJ, Bakker WH, Kooij PP, de Herder WW, Feelders RA, et al. Radiolabeled somatostatin analog [177Lu-DOTA0,Tyr3]octreotate in patients with endocrine gastroenteropancreatic tumors. J Clin Oncol 2005;23:2754–62.

[10] Kwekkeboom DJ, de Herder WW, Kam BL, van Eijck CH, van Essen M, Kooij PP, et al. Treatment with the radiolabeled somatostatin analog [177 Lu-DOTA 0,Tyr3]octreotate: Toxicity, efficacy, and survival. J Clin Oncol 2008;26:2124–30.

[11] Dieudonne A, Hobbs RF, Bolch WE, Sgouros G, Gardin I. Fine-resolution voxel S values for constructing absorbed dose distributions at variable voxel size. J Nucl Med 2010;51: 1600–7.
[12] Ljungberg M, Frey E, Sjogreen K, Liu X, Dewaraja Y, Strand SE. 3D absorbed dose calculations based on SPECT: Evaluation for 111-In/90-Y therapy using Monte Carlo simulations. Cancer Biother Radiopharm 2003;18:99–107.
[13] Wilderman SJ, Dewaraja YK. Method for fast CT/SPECT-Based 3D Monte Carlo absorbed dose computations in internal emitter therapy. IEEE Trans Nucl Sci 2007;54: 146–51.
[14] Ljungberg M, Sjögren-Gleisner K. The accuracy of absorbed dose estimates in tumours determined by quantitative SPECT: a Monte Carlo study. Acta Oncol 2011 Aug;50: 981–9.
[15] S.Y.F. Chu LPEaRBF [Internet]. The Lund/LBNL Nuclear Data Search. 1999 [cited 2011 Aug 23]. Available from: http://nucleardata.nuclear.lu.se/nucleardata/toi/
[16] Helisch A, Forster GJ, Reber H, Buchholz HG, Arnold R, Goke B, et al. Pre-therapeutic dosimetry and biodistribution of 86Y-DOTA-Phe1-Tyr3-octreotide versus 111In-pentetreotide in patients with advanced neuroendocrine tumours. Eur J Nucl Med Mol Imaging 2004;31:1386–92.
[17] Therasse P, Eisenhauer EA, Verweij J. RECIST revisited: A review of validation studies on tumour assessment. Eur J Cancer 2006;42:1031–9.
[18] Flux G, Bardies M, Chiesa C, Monsieurs M, Savolainen S, Strand SE, et al. Clinical radionuclide therapy dosimetry: The quest for the "Holy Gray". Eur J Nucl Med Mol Imaging 2007;34:1699–700.
[19] Behr TM, Sharkey RM, Juweid ME, Blumenthal RD, Dunn RM, Griffiths GL, et al. Reduction of the renal uptake of radiolabeled monoclonal antibody fragments by cationic amino acids and their derivatives. Cancer Res 1995;55: 3825–34.
[20] Rolleman EJ, Valkema R, de Jong M, Kooij PP, Krenning EP. Safe and effective inhibition of renal uptake of radiolabelled octreotide by a combination of lysine and arginine. Eur J Nucl Med Mol Imaging 2003;30:9–15.
[21] Jamar F, Barone R, Mathieu I, Walrand S, Labar D, Carlier P, et al. 86Y-DOTA0)-D-Phe1-Tyr3-octreotide (SMT487) – a phase 1 clinical study: Pharmacokinetics, biodistribution and renal protective effect of different regimens of amino acid co-infusion. Eur J Nucl Med Mol Imaging 2003;30:510–8.
[22] Valkema R, Pauwels SA, Kvols LK, Kwekkeboom DJ, Jamar F, de Jong M, et al. Long-term follow-up of renal function after peptide receptor radiation therapy with (90)Y-DOTA(0),Tyr(3)-octreotide and (177)Lu-DOTA(0), Tyr(3)-octreotate. J Nucl Med 2005;46(Suppl 1):83S–91S.
[23] Konijnenberg M, Melis M, Valkema R, Krenning E, de Jong M. Radiation dose distribution in human kidneys by octreotides in peptide receptor radionuclide therapy. J Nucl Med 2007;48:134–42.